NASA TECHNICAL NOTE

NASA TN D-2742

NASA TN D-2742

AN EXPERIMENTAL INVESTIGATION OF SUPPORT INTERFERENCE ON A BLUNT BODY OF REVOLUTION AT A MACH NUMBER OF APPROXIMATELY 20

by Charles G. Miller III

Langley Research Center
Langley Station, Hampton, Va.

NATIONAL AERONAUTICS AND SPACE ADMINISTRATION • WASHINGTON, D. C. • APRIL 1965

NASA TN D-2742

AN EXPERIMENTAL INVESTIGATION OF SUPPORT INTERFERENCE ON A BLUNT BODY OF REVOLUTION AT A MACH NUMBER OF APPROXIMATELY 20

By Charles G. Miller III

Langley Research Center
Langley Station, Hampton, Va.

NATIONAL AERONAUTICS AND SPACE ADMINISTRATION

For sale by the Office of Technical Services, Department of Commerce,
Washington, D.C. 20230 -- Price $2.00

AN EXPERIMENTAL INVESTIGATION OF SUPPORT INTERFERENCE ON A BLUNT BODY OF REVOLUTION AT A MACH NUMBER OF APPROXIMATELY 20

By Charles G. Miller III
Langley Research Center

SUMMARY

An investigation has been conducted in the Langley hotshot tunnel to determine the effects of support interference on the base pressure of a hemisphere cylinder with a ratio of length to base diameter of 1. With base pressure serving as the indication of support-interference effects, the parameters sting length, sting diameter, and shroud semiapex angle were examined. The investigation was performed at a free-stream Mach number of approximately 20 over a range of free-stream Reynolds numbers per foot from 3.00×10^5 to 4.65×10^5 at zero angle of attack.

With a shroud having a semiapex angle of 30° and diameter of 0.834 model base diameter, the base pressure coefficient was independent of ratios of sting length to model base diameter greater than 2. When a shroud of the same diameter, but having a 90° semiapex angle, was employed, the base pressure coefficient was independent of ratios of sting length to model base diameter greater than 3. For the range of ratios of sting diameter to model base diameter examined (0.250 to 0.625), no significant variation of the base pressure coefficient was observed. Base pressure measurements made at radial stations 0.375 and 0.271 model base diameters from the model axis of revolution showed that no significant radial pressure gradient existed between the radial stations examined. For all support parameters investigated, no effect on the model surface pressure immediately ahead of the base was noted.

With sting-length effects minimized in the present investigation, the base pressure of the hemisphere cylinder was approximately three times the free-stream static pressure; thus the base pressure coefficient based on free-stream conditions was positive. This result is a departure from results obtained in the supersonic regime; however, by utilizing the afterbody Mach number and Reynolds number at the outer edge of the boundary layer just ahead of the model base as comparison parameters and redefining the base pressure coefficient as a function of base and afterbody flow conditions, the base pressure coefficients obtained in the present investigation were brought into fair agreement with those of an investigation on base pressure conducted in the supersonic regime. Fair agreement was also obtained between the sting-length effects of this investigation and those of the previously mentioned supersonic investigation for which similar afterbody Mach number and Reynolds number existed immediately ahead of the model bases.

INTRODUCTION

In wind-tunnel investigations involving the measurement of model aerodynamic characteristics which are influenced by support geometry (e.g., base pressure and force studies), it is of considerable importance to minimize the effects of model support interference. Previous studies of support interference have demonstrated that even relatively small stings have some influence on the base pressure. For instance, as illustrated in reference 1, the base pressure of a sting-supported cone-cylinder model having a ratio of sting diameter to model base diameter of 0.4 was approximately 30 percent greater than the base pressure of the same model when magnetically suspended for a free-stream Mach number of approximately 7.6. Although many investigations of support interference have been made in the subsonic, transonic, and supersonic regimes (refs. 2 to 10), little research has been done in the hypersonic regime. Because of the scarcity of information on support interference in the hypersonic regime, an investigation was performed in the Langley hotshot tunnel to determine the effects of support interference on the base pressure of a blunt body of revolution.

With base pressure serving as the indication of support-interference effects, the parameters sting length, sting diameter, and shroud semiapex angle were examined. Data were obtained for four stings having ratios of sting diameter to model base diameter of 0.250, 0.375, 0.500, and 0.625 and ratios of sting length to model base diameter ranging from 1 to 8. The influence of shroud semiapex angle on critical sting length was observed for shroud angles of 30° and 90°. To gain an insight to the flow in the base region, the surface pressure distribution along the sting was measured. The tests were performed at a free-stream Mach number of approximately 20 over a range of free-stream Reynolds numbers per foot from 3.00×10^5 to 4.65×10^5.

SYMBOLS

C_p	pressure coefficient, $\frac{p - p_\infty}{q_\infty}$
d	sting diameter
D	model base diameter
f	fineness ratio (ratio of model length to model base diameter)
l	sting length
$\left(\frac{l}{D}\right)_{cr}$	ratio of critical sting length to model base diameter
L	model length

M	Mach number
p	pressure
q	dynamic pressure
R_a	afterbody Reynolds number per foot, $\frac{\rho_a U_a}{\mu_a}$
$R_{a,L}$	afterbody Reynolds number based on model length, $\frac{\rho_a U_a L}{\mu_a}$
R_∞	free-stream Reynolds number per foot, $\frac{\rho_\infty U_\infty}{\mu_\infty}$
$R_{\infty,L}$	free-stream Reynolds number based on model length, $\frac{\rho_\infty U_\infty L}{\mu_\infty}$
t	elapsed tunnel run time
T	temperature
U	velocity
x	distance along sting
α	angle of attack
β	wake angle
δ	boundary-layer thickness
μ	coefficient of viscosity
ρ	density
θ	shroud semiapex angle

Subscripts:

a	conditions on model afterbody (immediately ahead of model base)
b	conditions on model base
t,1	arc chamber conditions following arc discharge
t,2	stagnation conditions behind normal shock
∞	free-stream conditions

FACILITY AND APPARATUS

Facility and Tests

The Langley hotshot tunnel is a hypervelocity, arc-heated, blowdown wind tunnel. As shown in figure 1, the major components of this facility include a capacitor bank, an arc chamber, a 10° conical nozzle, a 24-inch cylindrical test section, a 10° cone-cylinder diffuser, and a vacuum reservoir. A more detailed description of this facility is presented in reference 11.

In the present investigation, with dry nitrogen as the test gas, the tunnel was operated at a free-stream Mach number of approximately 20 over a range of free-stream Reynolds numbers per foot from 3.00×10^5 to 4.65×10^5 which was assumed to result in laminar flow. Test-section pitot pressure and stagnation temperature were approximately 1 psi and 3000° K, respectively.

Model

The model used in this investigation was a 3-inch-diameter hemisphere cylinder with a fineness ratio of 1. As shown in figure 2, a single pressure orifice was located at the model nose for the measurement of stagnation pressure behind the normal shock. Two pressure orifices were located on the cylindrical afterbody to measure the surface pressure immediately ahead of the model base. For the purpose of measuring base pressure, the detachable model base was equipped with four pressure orifices located on a $1\frac{1}{8}$-inch-radius circle spaced 90° apart. In order to examine the possibility of a radial pressure distribution across the base, two pressure orifices were positioned on a 13/16-inch-radius circle spaced 180° apart.

Model Support System

The model and support system used in the present investigation are shown in figure 3 along with a tabulation of the support variables. A range of l/D of 1 to 8 was obtained by positioning the movable shroud to the desired location. Four 24-inch stings were utilized with $d/D = 0.250$, 0.375, 0.500, and 0.625 (fig. 4). Each sting was tested with a shroud of 90° semiapex angle and $2\frac{1}{2}$-inch diameter. The sting with $d/D = 0.375$ was also tested with a shroud of 30° semiapex angle and $2\frac{1}{2}$-inch diameter. The 15° shroud shown on the sting with $d/D = 0.500$ in figure 4 was not employed in the present investigation.

Instrumentation

The short running time of the tunnel (approximately 0.1 second) and low base pressures to be measured (0.001 to 0.006 psi) required pressure transducers

with very short response times, high sensitivity, and a minimum of orifice tube length. This in turn required a miniaturized pressure transducer that could be mounted within the model. A double-coil, single-diaphragm variable-reluctance pressure transducer (see ref. 12 for theory of operation) was employed in the present investigation. Geometric details of this transducer are shown in figure 5(a).

In order to calibrate the base pressure transducers while installed in the model, the transducers were referenced to an external vacuum source by a manifold housed within the model. This procedure allowed the reference pressure to be maintained at a constant level during the calibration. A typical calibration curve as shown in figure 5(b) was obtained by evacuating the tunnel and the reference manifold to approximately 0.0002 psi. The reference pressure being held constant, the pressure on the sensing side of the transducer was varied in desired increments with a tunnel bleed valve. Figure 6 illustrates the instrumentation of the model base and sting with the largest diameter. Although not shown, the transducers were wrapped in rubber to reduce mechanical vibrations during tunnel firing.

The initial charge pressure in the arc chamber was measured with a Bourdon type gage and upon arc discharge the chamber stagnation pressure was measured by two high-response strain-gage transducers. The model stagnation pressure behind the normal shock and afterbody surface pressure were measured with wafer-style variable reluctance transducers similar to those employed in measuring base pressure but having higher response time, lower sensitivity, and smaller size. (See refs. 12 and 13.) The transducers operating on the variable-reluctance principle were excited by 5-volt 20-kilocycle carrier amplifiers. The output signals from these amplifiers drove galvanometers in a light-beam type of oscillograph having a variety of chart speeds.

DATA REDUCTION AND ACCURACY

Data Reduction

A typical oscillograph record illustrating base, afterbody, pitot, and arc-chamber pressure traces is shown in figure 7. This record demonstrates the fast response of the gages, the low oscillatory level of the traces, the short starting transient time of the tunnel, and the relatively long usable running time. The net deflections in inches were read from the oscillograph traces at 10-millisecond intervals and then reduced to pressures using the respective calibration curves.

With the use of the arc-chamber conditions following arc discharge and the pitot pressure measured in the test section, test-section thermodynamic and aerodynamic properties were calculated by using the data-reduction program as presented in reference 14. Base pressures used in the present investigation represent the average measurement from the four orifices on the $1\frac{1}{8}$-inch-radius circle shown in figure 2.

Accuracy

Uncertainties involved in the instrumentation, readability of oscillograph records, and repeatability of test conditions caused maximum probable inaccuracies in the present data as follows:

p_a, percent	±5.0
p_b, percent	±15.0
p_∞, percent	±5.0
q_∞, percent	±5.0

RESULTS AND DISCUSSION

Effect of Sting Length

Ratios of sting length to model base diameter ranging from 1 to 8 were investigated at a free-stream Reynolds number per foot of 3.00×10^5 and a ratio of sting diameter to model base diameter of 0.375. The effect of sting length on the base pressure coefficient of the hemisphere cylinder model is shown in figure 8(a). With the present shroud of 90° semiapex angle, the base pressure coefficient was independent of sting length for $l/D > 3$. The 90° semiapex angle shroud was employed in order to obtain the maximum critical sting length (critical sting length was defined as the sting length below which the base pressure increased with a further decrease in sting length, as shown in fig. 8(a) by the sudden increase of the base pressure coefficient).

Figure 8(b) shows the afterbody pressure coefficient to be independent of all l/D values examined, even when subcritical.

Effect of Shroud Angle on Critical Sting Length

The effect of sting length on the base pressure coefficient of the hemisphere cylinder model was also examined with a 30° semiapex angle shroud having the same diameter as the 90° shroud discussed in the preceding section. Both shrouds were tested at a free-stream Reynolds number per foot of 3.00×10^5 and $d/D = 0.375$.

As previously noted, the base pressure coefficient was independent of sting lengths greater than 3 base diameters when the shroud of 90° semiapex angle was employed. Figure 8(a) shows that for the shroud of 30° semiapex angle, the base pressure coefficient was independent of sting lengths greater than 2 base diameters. Although tests involving only 2 different shroud angles are insufficient to appraise completely the variation of critical sting length with change in shroud angle, the results illustrate the need to consider such variation in the design of a support system for minimum interference.

Effect of Reynolds Number on Critical Sting Length

There is an absence of published data concerning support interference for the range of free-stream Reynolds numbers experienced in the present investigation. Thus a comparison of the present data with results obtained in the supersonic regime using free-stream Reynolds number as the correlation parameter was not possible.

Base pressure investigations in the supersonic regime, including support interference, were performed by Kavanau in the laminar flow regime (ref. 2) and the transitional flow regime (ref. 3) over ranges of free-stream Reynolds numbers per foot from 1.88×10^3 to 4.44×10^4 and 9.36×10^5 to 2.46×10^6, respectively. Results from these studies taken directly from the respective references are shown in figure 9(a) in which a ratio of critical sting length to model base diameter is plotted as a function of free-stream Reynolds number based on model length. The models and sting configurations utilized by Kavanau and the present investigation are illustrated in the sketches of figure 9. Data points representing the critical sting length obtained in the present investigation for the 30° and 90° semiapex angle shrouds are also shown in figure 9(a).

As discussed in reference 15, when the reference Reynolds number is based on free-stream properties, the results can be especially misleading when blunt bodies are involved. Therefore, in order to compare the data of the present investigation with that of Kavanau, the flow properties at the outer edge of the boundary layer immediately ahead of the model base were examined for both investigations.

A surface pressure distribution on the 0.6-inch-diameter cone-cylinder model employed in reference 2 showed the afterbody surface pressure at 3.32 base diameters downstream of the model nose to be 0.755 free-stream pressure at a free-stream Mach number of 2.20. Calculations based on the ratio of this afterbody surface pressure to the stagnation pressure behind the shock, isentropic flow and perfect fluid relationships being assumed (ref. 16), gave an afterbody Mach number of 2.04. The afterbody temperature at the outer edge of the boundary layer was calculated to be approximately free-stream temperature ($T_a/T_\infty = 1.075$). Thus approximately, free-stream Mach number and three-fourths free-stream unit Reynolds number existed at the outer edge of the boundary layer just ahead of the base of the models utilized in reference 2.

With the afterbody surface pressure of the hemisphere cylinder employed in the present investigation and the measured pitot pressure, the afterbody flow conditions were determined. The afterbody Mach number ($M_a \approx 3.05$) and the afterbody Reynolds number based on model length fell into the range of afterbody flow conditions experienced by Kavanau in reference 2 as shown in figure 9(b).

The data of figure 9(b) demonstrate an improved correlation from that shown in figure 9(a) between the present investigation and that of reference 2. The validity of such a correlation is supported by reference 17. Basing the Reynolds number on conditions at the outer edge of the boundary layer

immediately ahead of the model base helps to indicate the flow condition just before separation to form the wake. However, it should be noted that the boundary layer of the cone-cylinder model in reference 2 was near adiabatic wall conditions whereas the boundary layer of the hemisphere-cylinder model used in the present investigation was being cooled by the model. Since the flow over the model base is a function of boundary-layer conditions, perfect agreement between the two investigations would not be expected. Another factor concerning the agreement of the present data with that of reference 2 is that Kavanau found the shroud diameter to have an appreciable effect on critical sting length at low Reynolds number. In reference 2, Kavanau employed a shroud diameter of 2.1 model base diameters whereas the shroud used in the present investigation was 0.834 model base diameter. Kavanau also found critical sting length to be dependent upon d/D. The effects of sting diameter on the base pressure coefficient in the present investigation and reference 2 will be discussed in a following section.

From figure 9(b) a corresponding plot of the ratio of critical sting length to model base diameter as a function of unit Reynolds number based on afterbody flow conditions was obtained and is shown in figure 9(c). The present data is observed to fall in the approximate region where a curve representing an interpolation of the $M_a \approx 2.10$ and $M_a \approx 4.00$ data of reference 2, for $M_a \approx 3.05$, would be expected. Individual curves obtained for the geometrically identical models of different scaling of reference 2, tested at the same free-stream conditions, illustrate the influence of boundary layer on sting-length effects. As mentioned previously, the differences of boundary-layer conditions just upstream of the base for the present investigation and reference 2 would imply that the agreement shown by figure 9(c) is coincidental.

Effect of Sting Diameter

The results of the sting-diameter tests which were performed at a free-stream Reynolds number per foot of 4.11×10^5, a sting length of 3 base diameters, and a shroud semiapex angle of 90° are presented in figure 10. Figure 10(a) shows no significant variation in the base pressure coefficient over the d/D range (0.250 to 0.625) examined. Kavanau (ref. 2) observed a linear increase in base pressure with increasing sting diameter, the base pressure being approximately 25 percent greater for the maximum d/D value examined (0.5) when compared with the minimum ratio examined (0.07).

The afterbody pressure coefficient was not influenced by variation in sting diameter as demonstrated by figure 10(b). Afterbody pressures were not measured when the sting diameter of 0.250 base diameter was utilized because of the lack of sting cross-sectional area for instrumentation leads.

Pressure Distribution Across Model Base

Base pressure measurements were made at radial stations 0.375 and 0.271 model base diameters from the model axis. From figure 11 it can be observed that no significant radial pressure gradient existed between the radial

stations examined. The findings of reference 2 showed the base pressure at a radial station of 0.271 base diameter to be 1.3 times the base pressure at a radial station of 0.375 base diameter for a wire-supported model tested at $M_\infty = 3.9$.

Model and Sting Surface Pressure Distribution

Because of the low density of the base flow, attempts to observe the wake with a single-pass schlieren system proved unsuccessful. To gain an insight to the flow over the model base, a pressure distribution on the afterbody and along the sting surface was obtained as shown in figure 12. This investigation was conducted at a free-stream Reynolds number per foot of 4.65×10^5, $d/D = 0.625$, $l/D = 3$, and $\theta = 90^\circ$.

As shown in figure 12, the afterbody pressure just ahead of the model base was observed to be approximately 5 times the base pressure. In the present investigation of the effect of sting length, the afterbody pressure was always greater than the base pressure even for subcritical sting lengths. Figure 8(b) illustrates that the afterbody pressure just ahead of the model base was independent of all l/D values examined.

At 0.167 base diameter downstream of the base, the pressure measured on the sting surface is approximately equal to the base pressure. However, at 0.66 base diameter, the static pressure increases to approximately 3 times the base pressure. Thus the conical expansion about the model base creates a cavity region of low-energy flow characterized at the downstream end by a recompression region caused by the convergence of the wake. (See fig. 12.) This recompression region, which occurs in the vicinity of the narrowest portion of the wake, is usually denoted as the "critical region" or "throat" (refs. 2, 4, and 5). In order to approximate the region of flow reattachment to the sting, a Prandtl-Meyer expansion to the pressure measured 0.167 base diameter downstream of the base was performed. This calculation yielded a wake angle β of approximately 17° and a reattachment point at 0.60 base diameter downstream of the base. Although scarcity of sting-surface pressure measurements between the model base and 1.0 base diameter downstream of the base prohibited the accurate determination of the sting station of maximum pressure because of flow reattachment, the qualitative agreement between the calculated Prandtl-Meyer expansion and the pressure measured at 0.66 base diameter downstream of the base serves to approximate the region of flow reattachment to the sting.

Downstream of the region of flow reattachment to the sting, the sting surface pressure is observed to decay linearly toward the free-stream static pressure. (See dashed line of fig. 12.) However, beyond 2.33 base diameters the sting surface pressure increases sharply. This pressure rise is associated with the flow separation about the shroud. As shown by the dashed line of figure 12, an axial variation in free-stream static pressure exists but is of such magnitude that the effects associated with this variation are essentially negligible.

According to the theory of Crocco and Lees, disturbances downstream of the throat are unable to affect the flow upstream (refs. 2, 4, and 5). However, Whitfield (refs. 4 and 5) showed that for the transitional wake case the throat does not represent the limit of approach of a shroud to the model base without interference. The data of Whitfield indicated that the 20° semiapex angle shroud having a ratio of shroud diameter to model base diameter of 2.0 should be positioned 1.0 to 1.5 base diameters downstream of the throat to eliminate sting-length effects. Reference 6 states, for the turbulent case, that a shroud having a semiapex angle no greater than 20° should be stationed approximately 0.85 base diameter downstream of the throat. From figure 10(a) the wake angle of the hemisphere cylinder employed in the present investigation was assumed to be essentially constant for variation in sting diameter. Thus the results of the present investigation, in which laminar flow is assumed, show that a 30° semiapex angle shroud having a diameter approximately that of the model should be positioned 1 base diameter downstream of the throat to eliminate sting-length effects.

Base Pressure

In the present investigation, the base pressure was observed to be approximately 3 times the free-stream static pressure (fig. 12). This results in a positive base pressure coefficient which is a departure from results obtained in base pressure and support interference studies in the supersonic and low hypersonic regimes (refs. 1 to 10). Reference 1 shows the base pressure of a sting-supported cone-cylinder model having $d/D = 0.4$ to be approximately 30 percent greater than the base pressure experienced by the same model when magnetically suspended for $M_\infty \approx 7.6$ and laminar boundary layer. The magnitude of this increase in base pressure due to a sting (ref. 1) and the trend indicated in figure 10(a) of the present investigation imply that the base pressure of the present hemisphere-cylinder model for the present free-stream flow conditions would be greater than free-stream static pressure if tested under free flight. This is in accordance with the prediction of Ferri and Pallone (ref. 18) that at high hypersonic Mach numbers the pressure on the base of a blunt body is greater than the free-stream static pressure.

If the ratio of base pressure to free-stream static pressure from the present investigation is plotted as a function of free-stream Reynolds number based on model length and compared with results of reference 2, results similar to those shown in figure 9(a) would occur. However, by utilizing the afterbody Mach number and Reynolds number at the outer edge of the boundary layer just ahead of the model base as comparison parameters and redefining the base pressure coefficient as a function of base and afterbody flow conditions, the discrepancy between the pressure coefficients obtained in the present investigation and those of reference 2 was decreased. This effect is demonstrated in figure 13(a) where the ratio of base pressure to afterbody surface pressure just ahead of the model base is plotted as a function of afterbody Reynolds number based on model length. Justification for the comparison of data of reference 2 with the present data on the basis of afterbody conditions was discussed previously. Again, perfect agreement is not expected because of the differences of boundary-layer conditions experienced by the models of the respective investigations.

Figure 13(b), where the ratio of base pressure to afterbody surface pressure just ahead of the model base is plotted as a function of unit Reynolds number based on afterbody flow conditions, shows good agreement between the present data and Kavanau's data for the 0.3-inch-diameter model. This agreement, supported by figure 9(c), would seem to imply that if the base pressure coefficient is defined as a function of base and afterbody flow conditions and afterbody unit Reynolds number and Mach number are used as correlation parameters, a correlation of base pressure data obtained in the supersonic regime would be possible with data obtained in the hypersonic regime. However, because of the differences in boundary-layer conditions, coincidental agreement is suspected and therefore more data must be obtained on this matter to validate such a comparison.

CONCLUSIONS

An investigation of support interference on the base pressure of a hemisphere cylinder with variation in sting length, sting diameter, and shroud semiapex angle (constant shroud diameter of 0.834 model base diameter) at a free-stream Mach number of approximately 20 over a range of free-stream Reynolds numbers per foot from 3.00×10^5 to 4.65×10^5 at zero angle of attack led to the following conclusions:

1. For a shroud semiapex angle of 90°, the base pressure coefficient was independent of ratios of sting length to model base diameter greater than 3, but may be reduced to 2 for a 30° semiapex angle shroud.

2. Variation in ratios of sting diameter to model base diameter from 0.250 to 0.625 had no significant influence on the base pressure coefficient.

3. Base pressure measurements at radial stations 0.375 and 0.271 model base diameters from the model axis of revolution showed that no significant radial pressure gradient existed between the radial stations examined.

4. Pressures on the model surface immediately ahead of the base were independent of all support parameters examined.

5. Fair agreement was obtained between the sting-length effects and ratios of base pressure to afterbody surface pressure of this investigation with a supersonic investigation for which similar Reynolds number and Mach number existed immediately ahead of the model base.

6. Base pressure of the sting supported hemisphere-cylinder model of fineness ratio 1 was found to be approximately 3 times the free-stream static pressure, a departure from results obtained in the supersonic regime.

Langley Research Center,
National Aeronautics and Space Administration,
Langley Station, Hampton, Va., December 2, 1964.

REFERENCES

1. Dubois, Georges; and Rogué, Charles: Sur une méthode de mesure de la pression de culot - Mesure et visualisation sur une maquette cylindro-conique suspendue magnétiquement a $M_o \simeq 7,6$. (On a Method for Measuring the Base Pressure - Measurement and Visualization on a Cone Cylinder Magnetically Suspended at $M_o \simeq 7.6$). La Recherche Aéronautique (O.N.E.R.A.), no. 79, Nov.-Dec. 1960, pp. 35-44.

2. Kavanau, L. L.: Base Pressure Studies in Rarefied Supersonic Flows. Rept. No. HE-150-125 (Contract N7-onr-295-Task 3), Inst. Eng. Res., Univ. of California, Nov. 1, 1954.

3. Kavanau, L. L.: Results of Some Base Pressure Experiments at Intermediate Reynolds Numbers With M = 2.84. Rept. No. HE-150-117 (Contract N7-onr-295-Task 3), Inst. Eng. Res., Univ. of California, Oct. 22, 1953.

4. Whitfield, Jack D.: Critical Discussion of Experiments on Support Interference at Supersonic Speeds. AEDC-TN-58-30, ASTIA Doc. No. AD-201108, U.S. Air Force, Aug. 1958.

5. Whitfield, Jack D.: Support Interference at Supersonic Speeds. AGARD Rept. 300, Mar. 1959.

6. Love, E. S.: A Summary of Information on Support Interference at Transonic and Supersonic Speeds. NACA RM L53K12, 1954.

7. Chapman, Dean R.: An Analysis of Base Pressure at Supersonic Velocities and Comparison With Experiment. NACA Rep. 1051, 1951. (Supersedes NACA TN 2137.)

8. Perkins, Edward W.: Experimental Investigation of the Effects of Support Interference on the Drag of Bodies of Revolution at a Mach Number of 1.5. NACA TN 2292, 1951. (Supersedes NACA RM A8B05.)

9. Reller, John O., Jr.; and Hamaker, Frank M.: An Experimental Investigation of the Base Pressure Characteristics of Nonlifting Bodies of Revolution at Mach Numbers From 2.73 to 4.98. NACA TN 3393, 1955. (Supersedes NACA RM A52E20.)

10. Lee, George; and Summers, James L.: Effects of Sting-Support Interference on the Drag of an Ogive-Cylinder Body With and Without a Boattail at 0.6 to 1.4 Mach Number. NACA RM A57I09, 1957.

11. Smith, Fred M.; Harrison, Edwin F.; and Lawing, Pierce L.: Description and Initial Calibration of the Langley Hotshot Tunnel With Some Real-Gas Charts for Nitrogen. NASA TN D-2023, 1963.

12. Smotherman, W. E.: A Miniature Wafer-Style Pressure Transducer. AEDC-TR-60-11, U.S. Air Force, Oct. 1960.

13. Smotherman, W. E.; and Maddox, W. V.: Variable Reluctance Pressure Transducer Development. AEDC-TDR-63-135, U.S. Air Force, July 1963.

14. Grabau, Martin; Humphrey, Richard L.; and Little, Wanda J.: Determination of Test-Section, After-Shock, and Stagnation Conditions in Hotshot Tunnels Using Real Nitrogen at Temperatures From 3000 to 4000° K. AEDC-TN-61-82, U.S. Air Force, July 1961.

15. Whitfield, Jack D.; and Potter, J. Leith: On Base Pressures at High Reynolds Numbers and Hypersonic Mach Numbers. AEDC-TN-60-61, U.S. Air Force, Mar. 1960.

16. Ames Research Staff: Equations, Tables, and Charts for Compressible Flow. NACA Rept. 1135, 1953. (Supersedes NACA TN 1428.)

17. Kuehn, Donald M.: Laminar Boundary-Layer Separation Induced by Flares on Cylinders at Zero Angle of Attack. NASA TR R-146, 1962.

18. Ferri, Antonio; and Pallone, Adrian: Note on the Flow Fields on the Rear Part of Blunt Bodies in Hypersonic Flow. WADC Tech. Note 56-294, U.S. Air Force, July 1956.

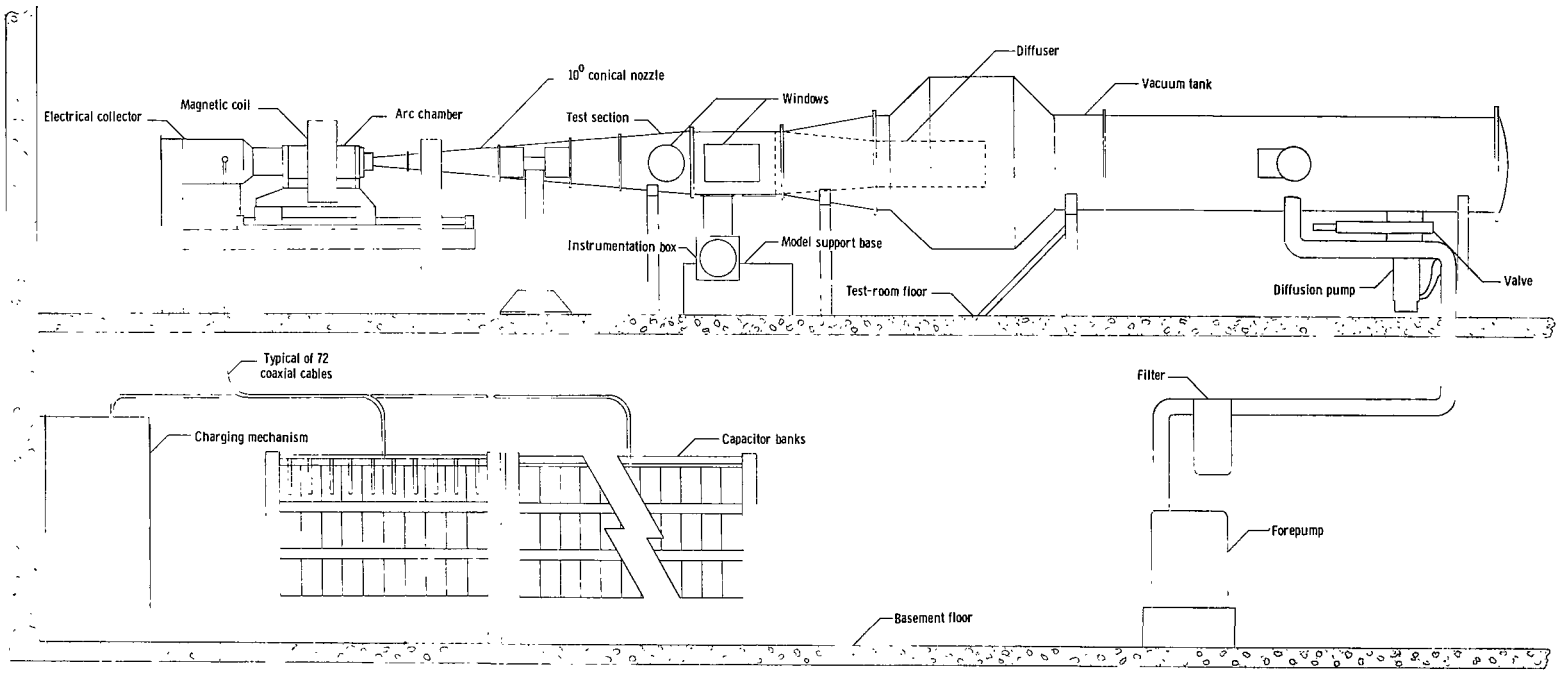

Figure 1.- Elevation of the Langley hotshot tunnel.

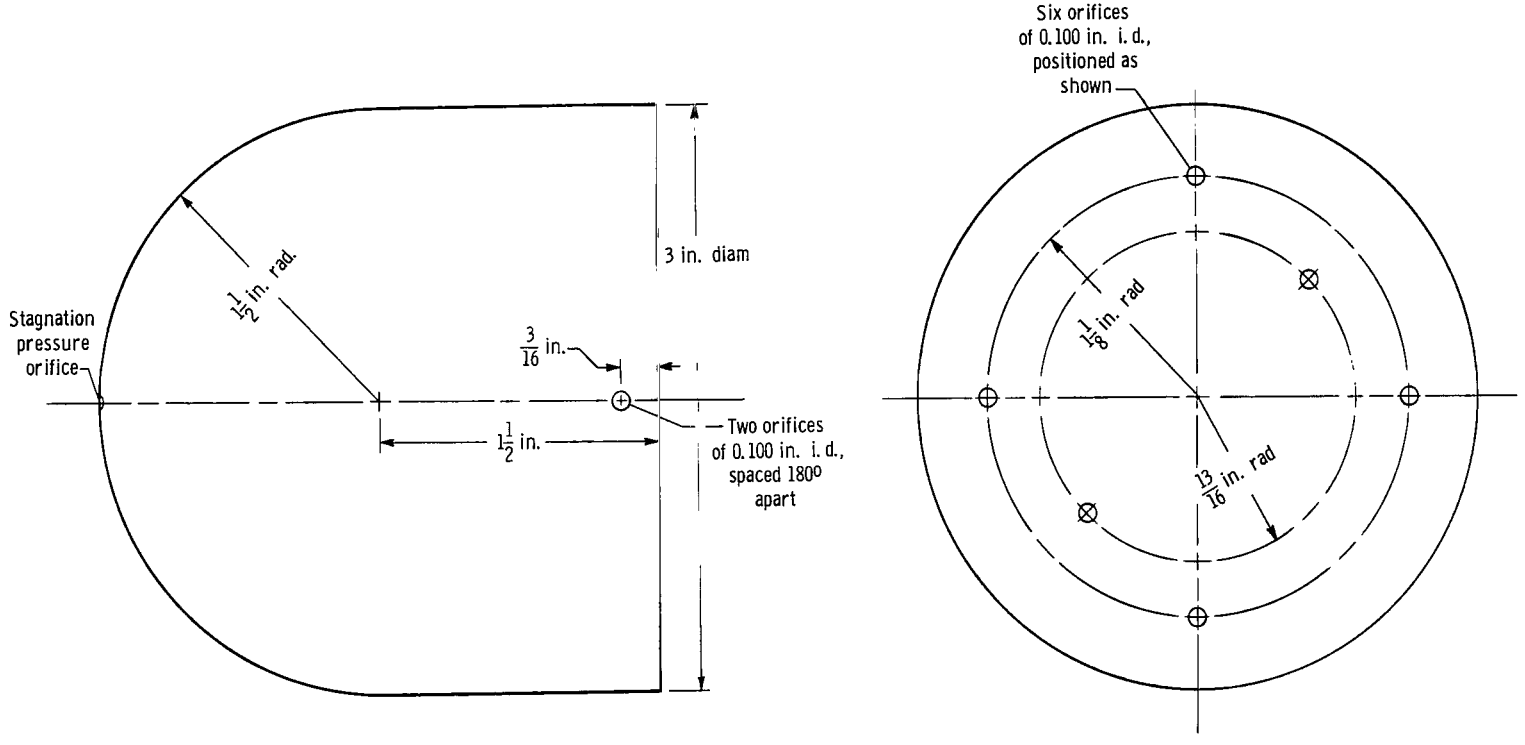

Figure 2.- Model geometry illustrating the location of base and afterbody pressure orifices.

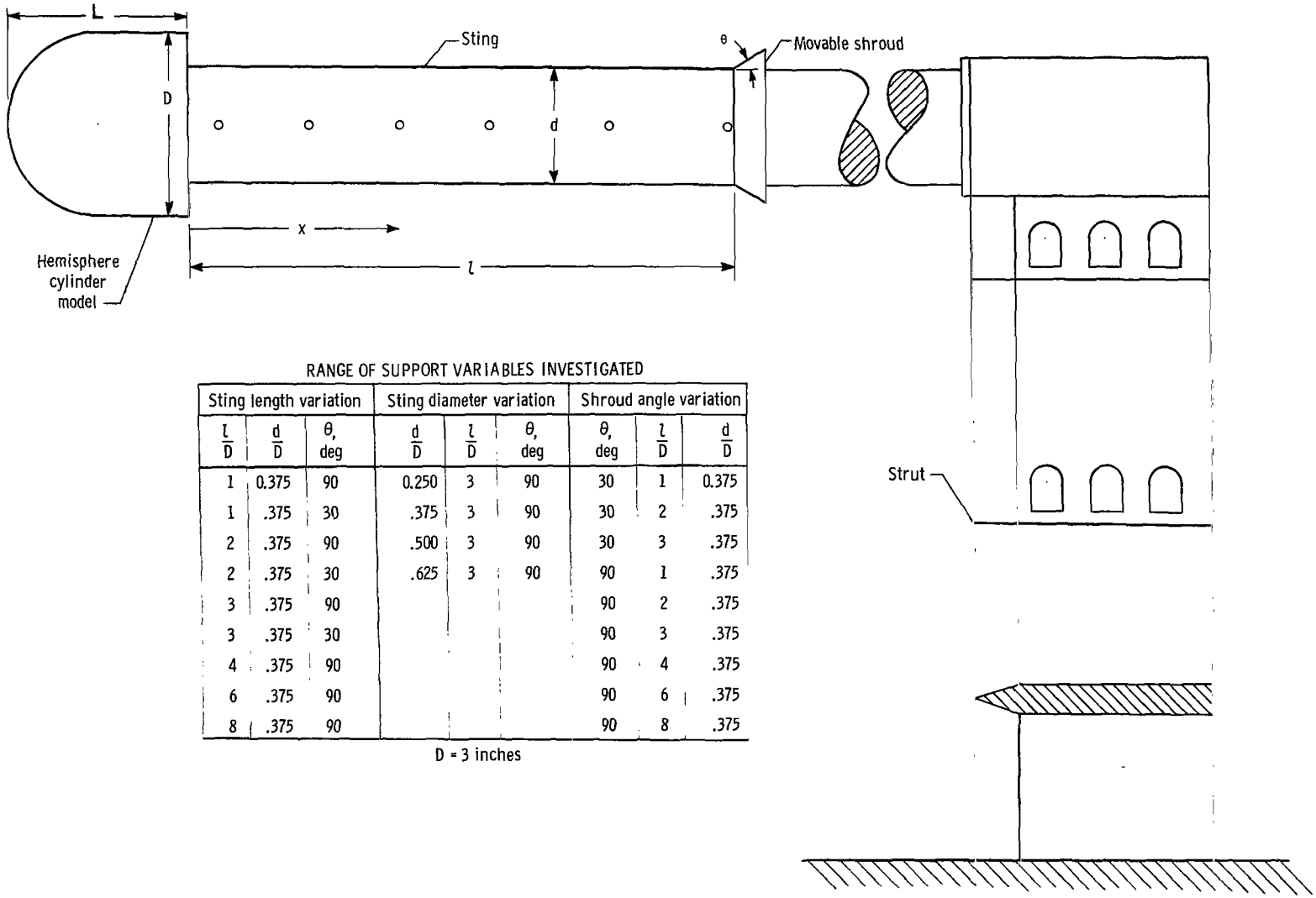

RANGE OF SUPPORT VARIABLES INVESTIGATED

Sting length variation			Sting diameter variation			Shroud angle variation		
$\frac{l}{D}$	$\frac{d}{D}$	θ, deg	$\frac{d}{D}$	$\frac{l}{D}$	θ, deg	θ, deg	$\frac{l}{D}$	$\frac{d}{D}$
1	0.375	90	0.250	3	90	30	1	0.375
1	.375	30	.375	3	90	30	2	.375
2	.375	90	.500	3	90	30	3	.375
2	.375	30	.625	3	90	90	1	.375
3	.375	90				90	2	.375
3	.375	30				90	3	.375
4	.375	90				90	4	.375
6	.375	90				90	6	.375
8	.375	90				90	8	.375

D = 3 inches

Figure 3.- Model support system used in the investigation of support interference.

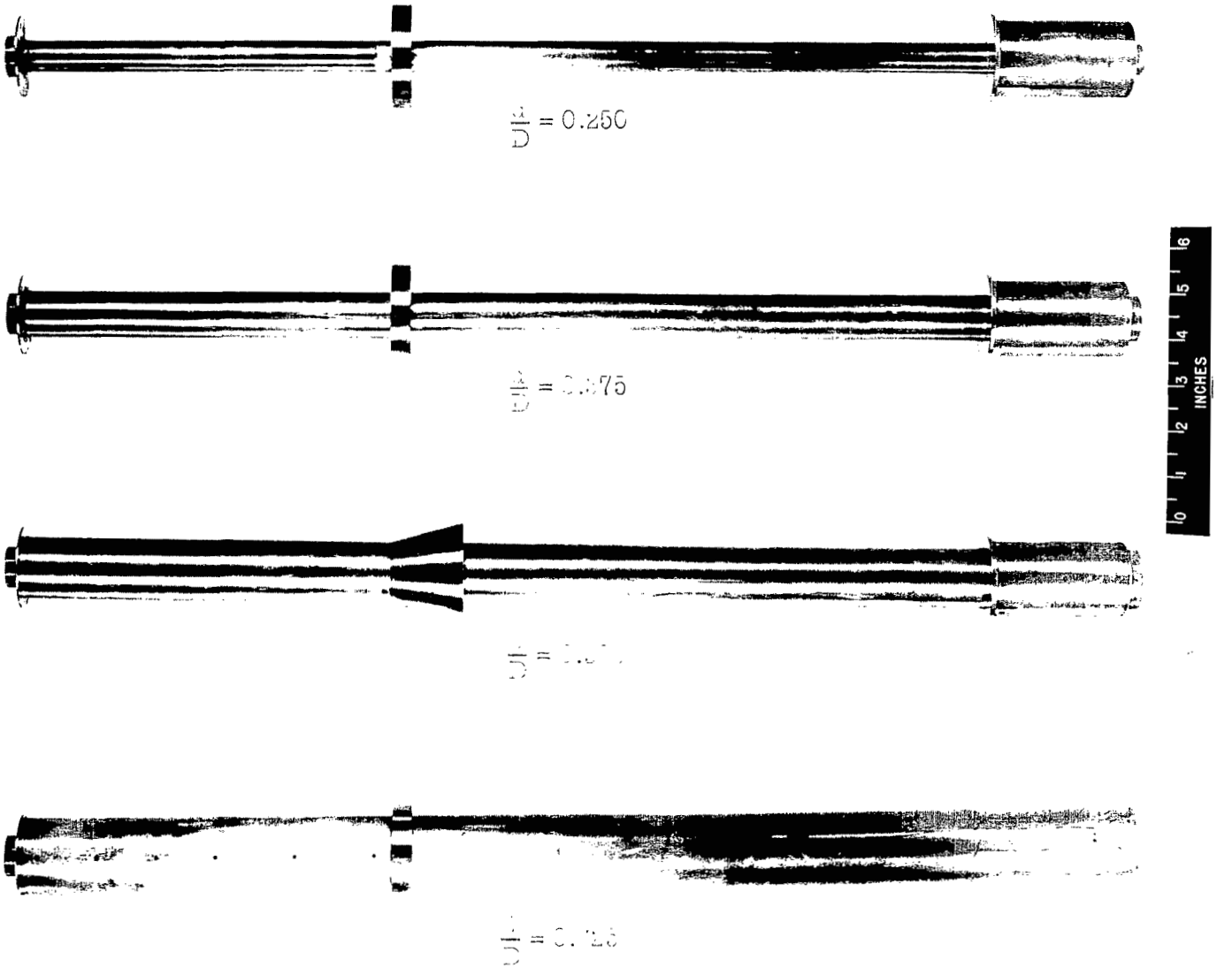

L-63-9695.1

Figure 4.- Various diameter stings used in present investigation.

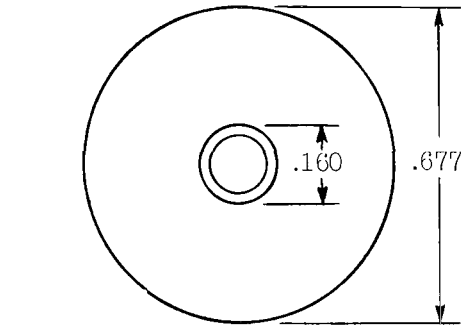

Top view

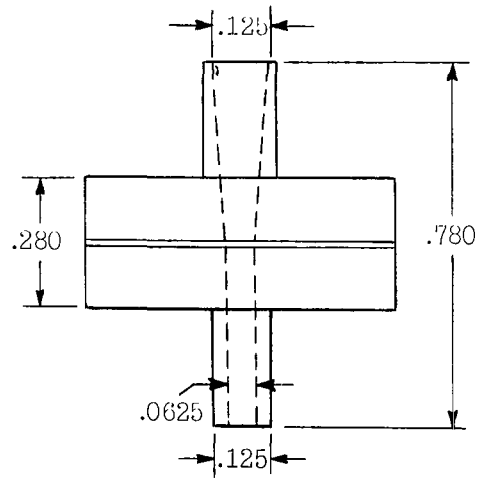

Side view

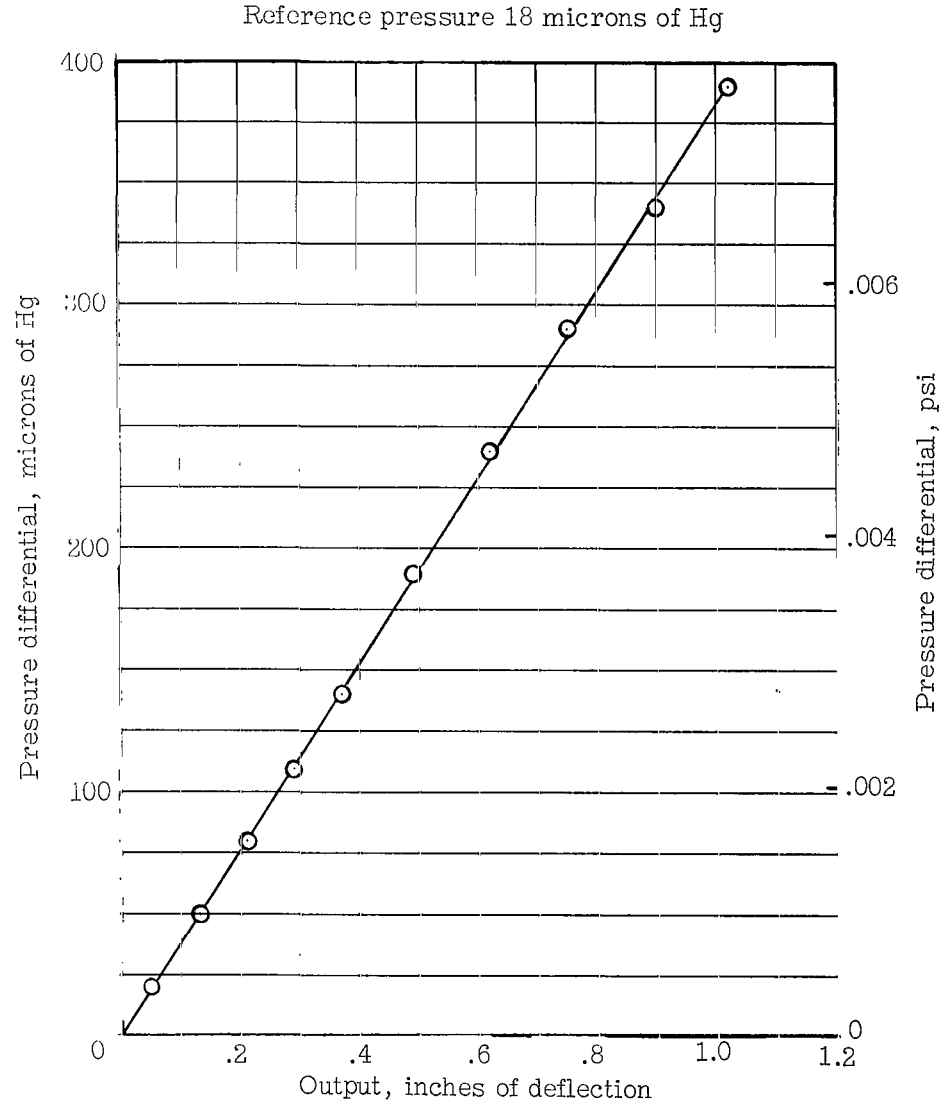

(a) Geometric detail. (All dimensions are in inches.)

(b) Typical calibration curve.

Figure 5.- Variable reluctance pressure transducer.

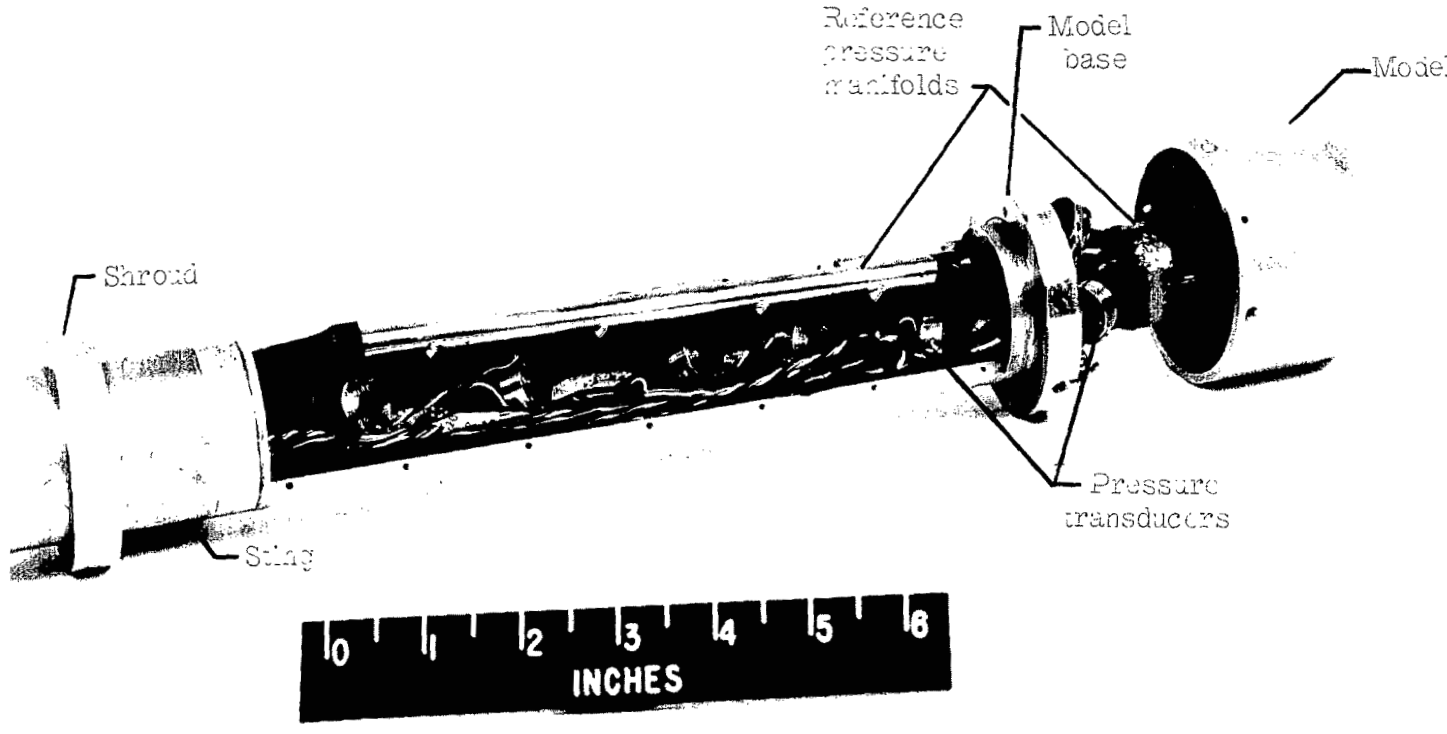

Figure 6.- Model and instrumented model base and sting. L-63-10063.1

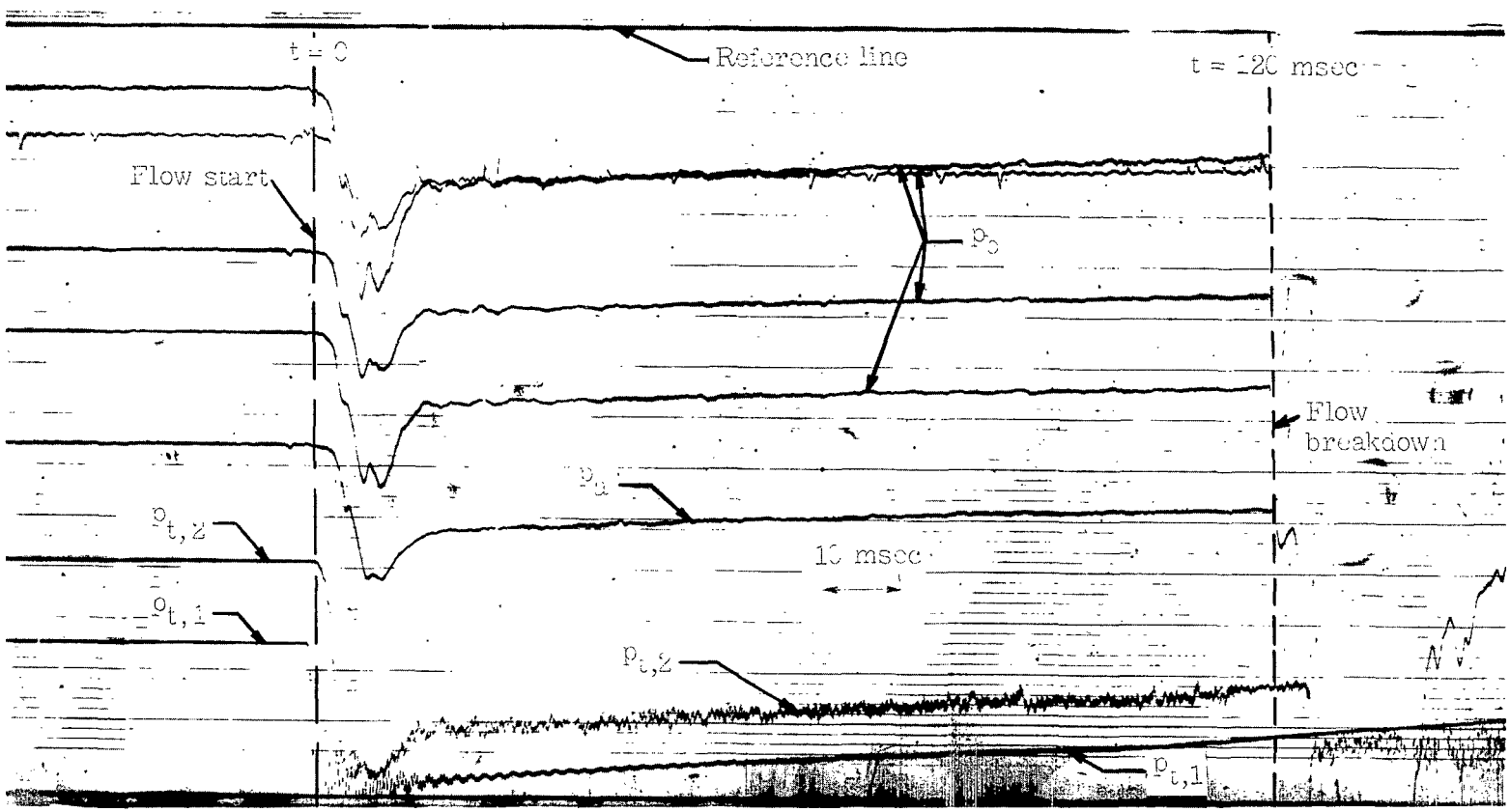

Figure 7.- Typical oscillograph record obtained in the present investigation of support interference.

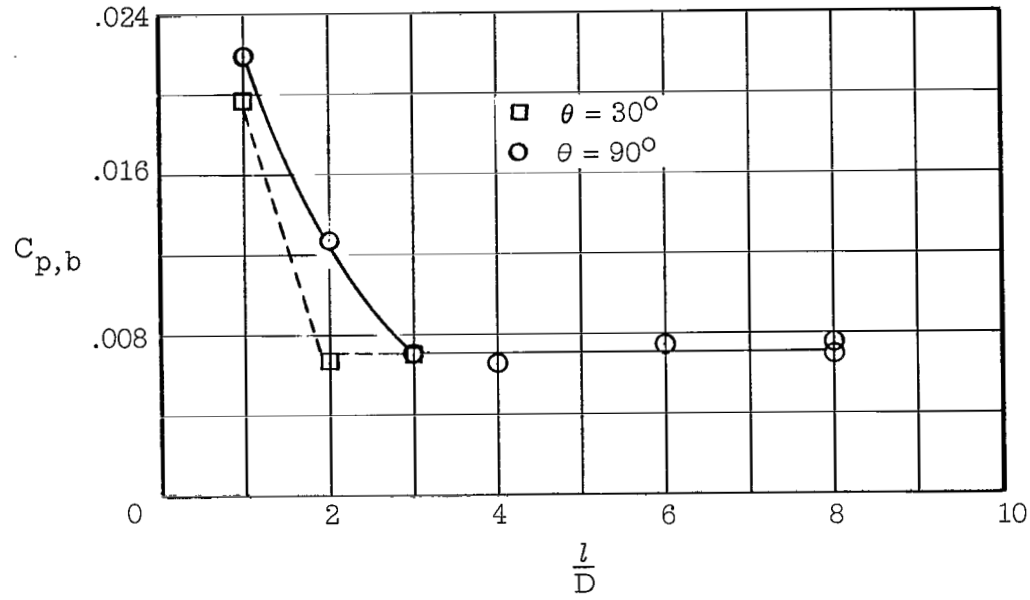

(a) Base pressure coefficient.

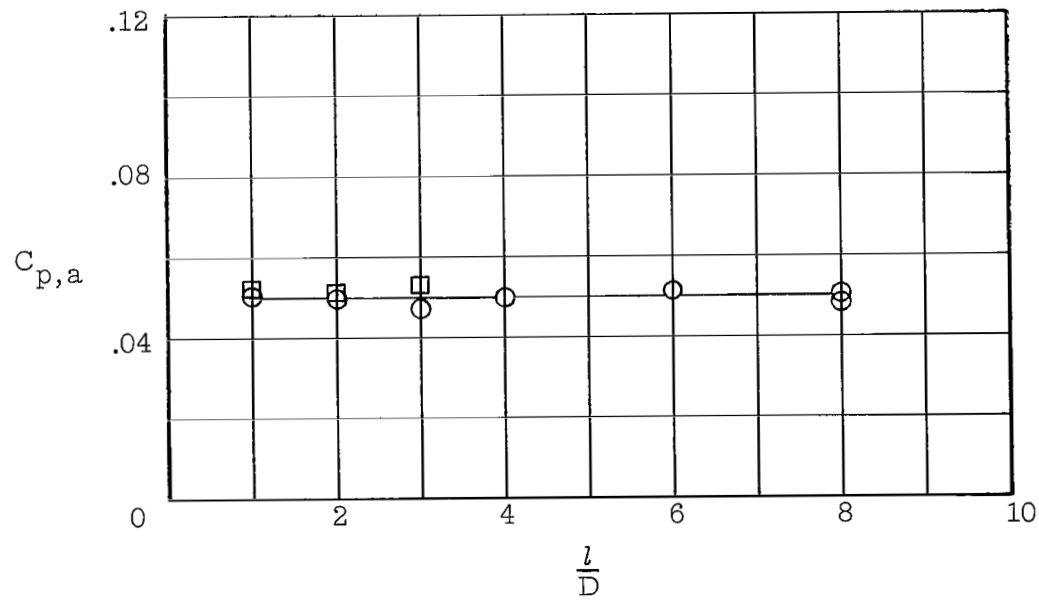

(b) Afterbody pressure coefficient.

Figure 8.- Effect of sting length on pressure coefficients of hemisphere cylinder. $R_{\infty} = 3.00 \times 10^5$ per foot, $d/D = 0.375$.

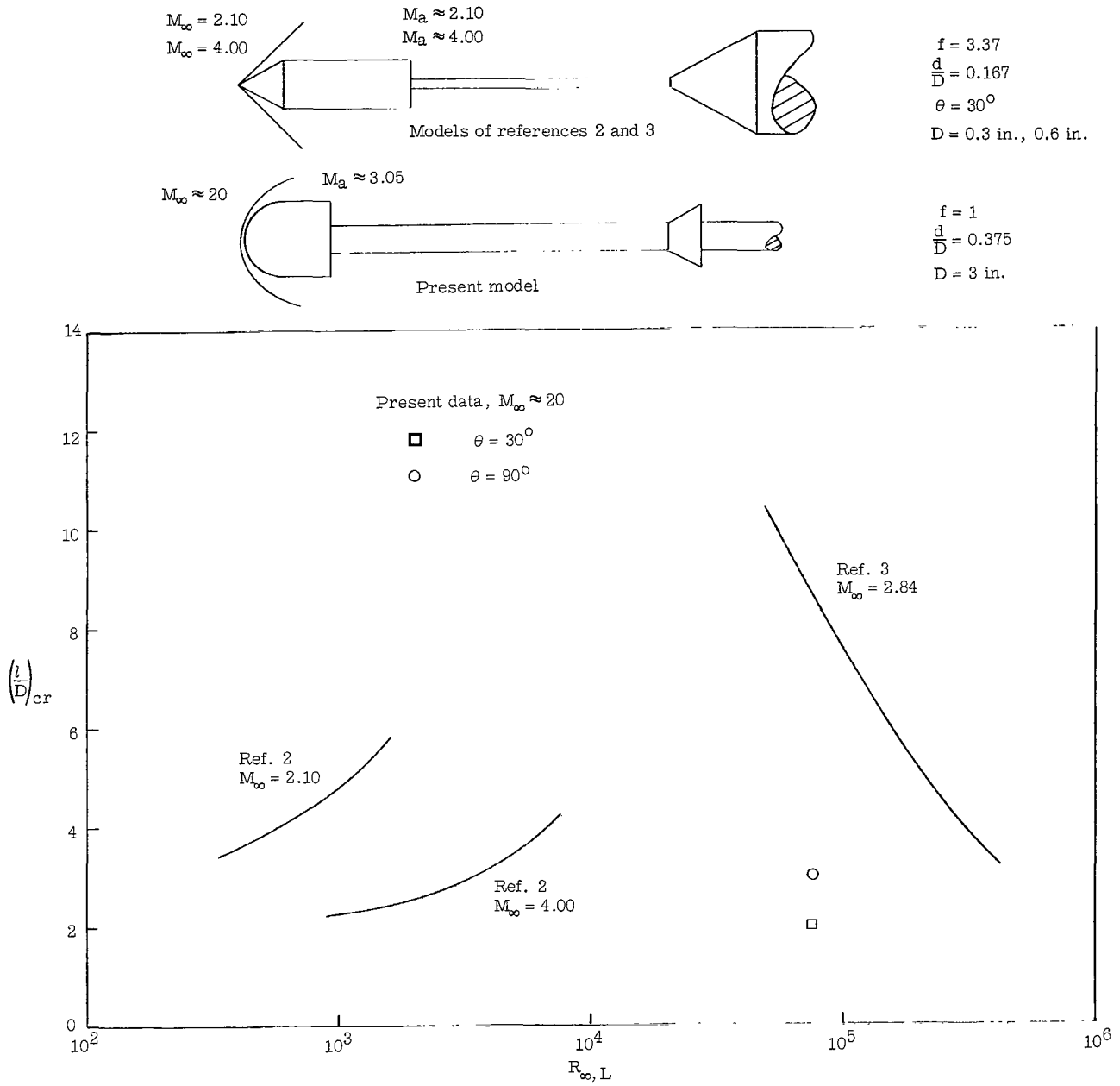

(a) Free-stream Reynolds number based on model length.

Figure 9.- Effect of Reynolds number on critical sting length.

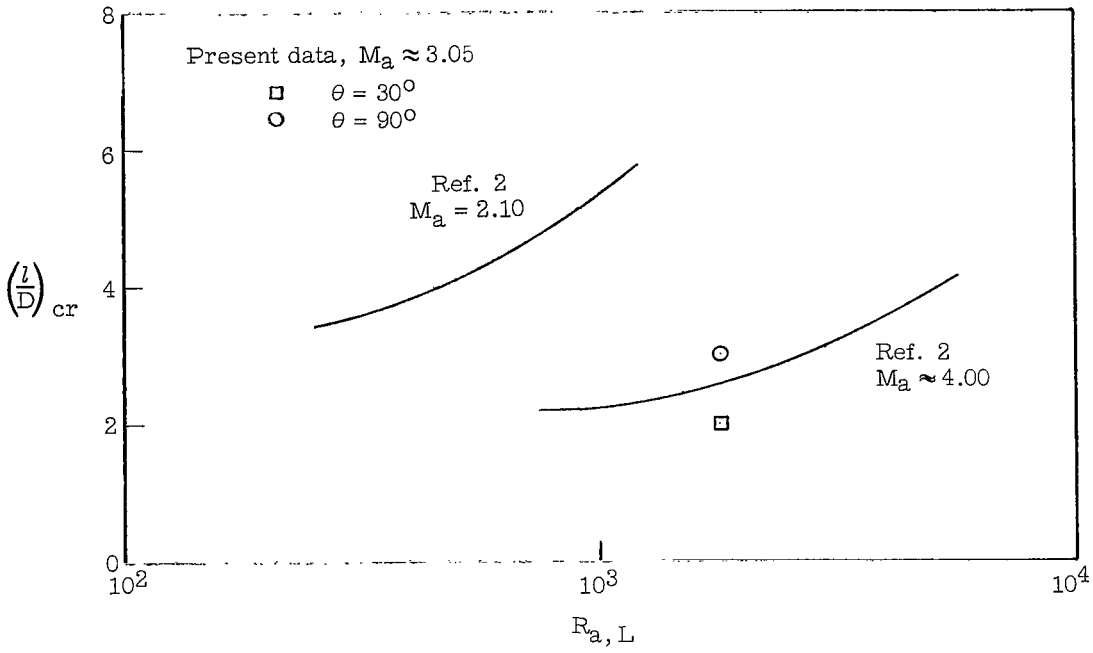

(b) Afterbody Reynolds number based on model length.

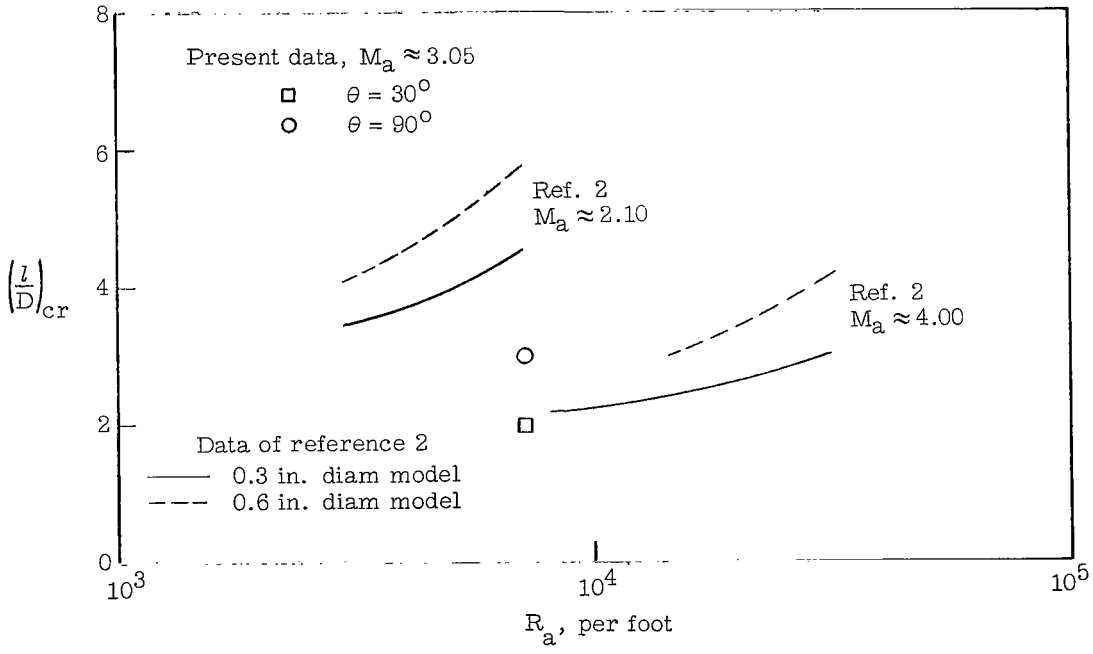

(c) Unit afterbody Reynolds number.

Figure 9.- Concluded.

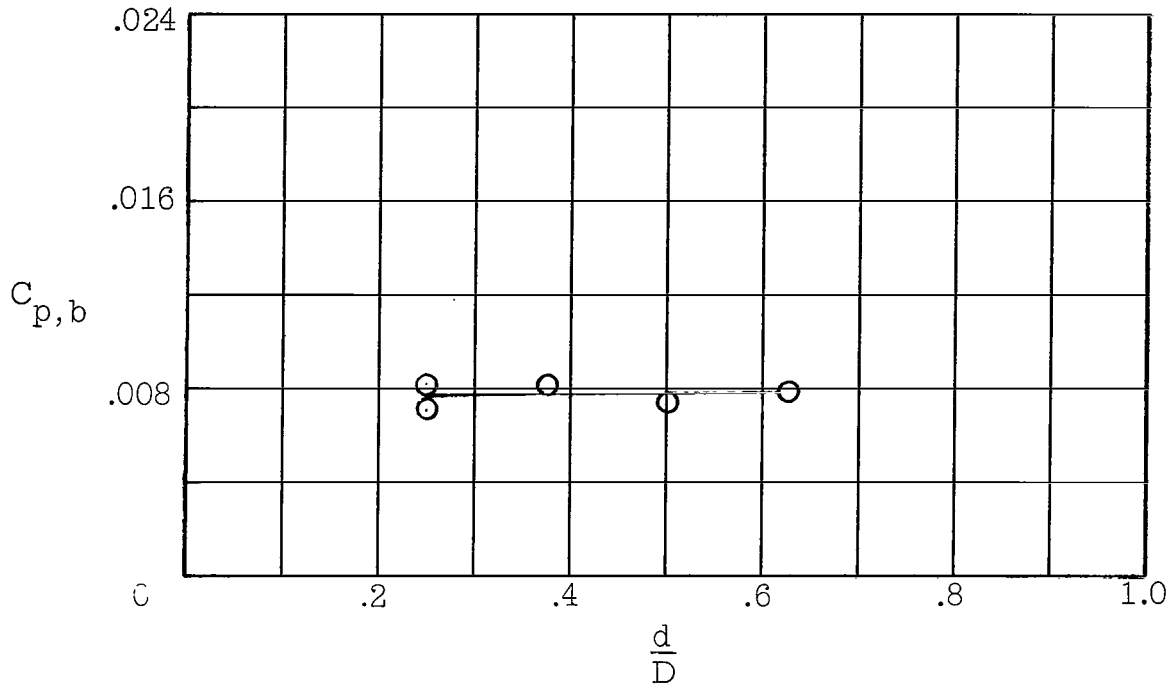

(a) Base pressure coefficient.

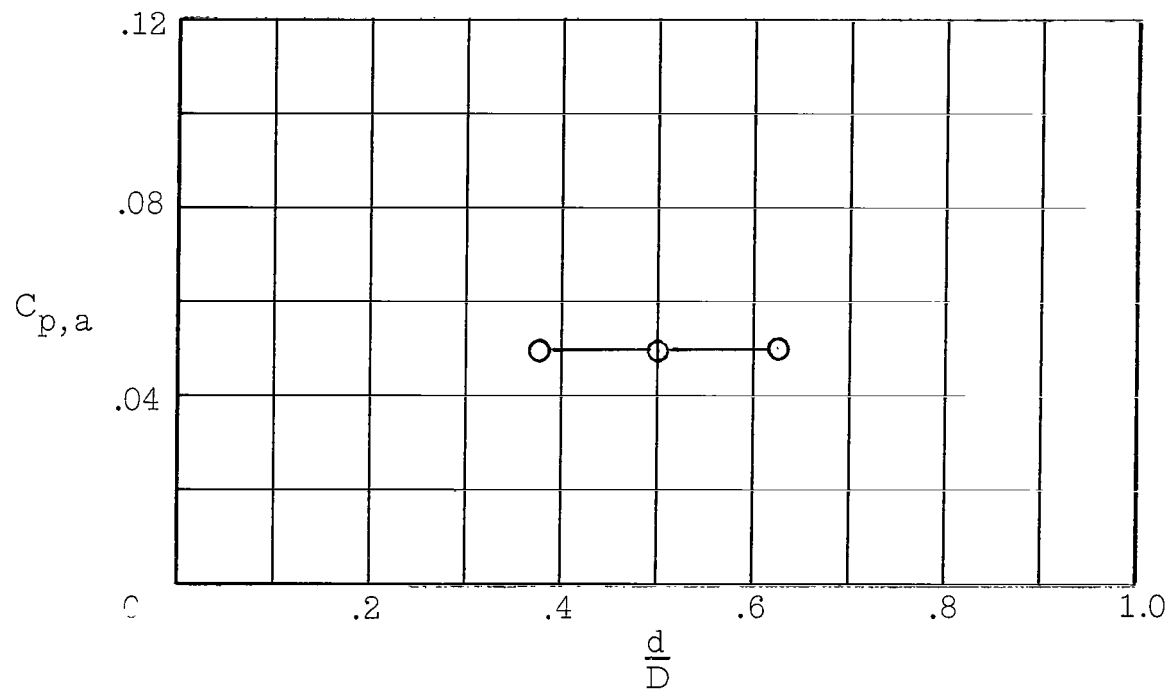

(b) Afterbody pressure coefficient.

Figure 10.- Effect of sting diameter on pressure coefficients of hemisphere cylinder model. $R_\infty = 4.11 \times 10^5$ per foot, $l/D = 3$; $\theta = 90^\circ$.

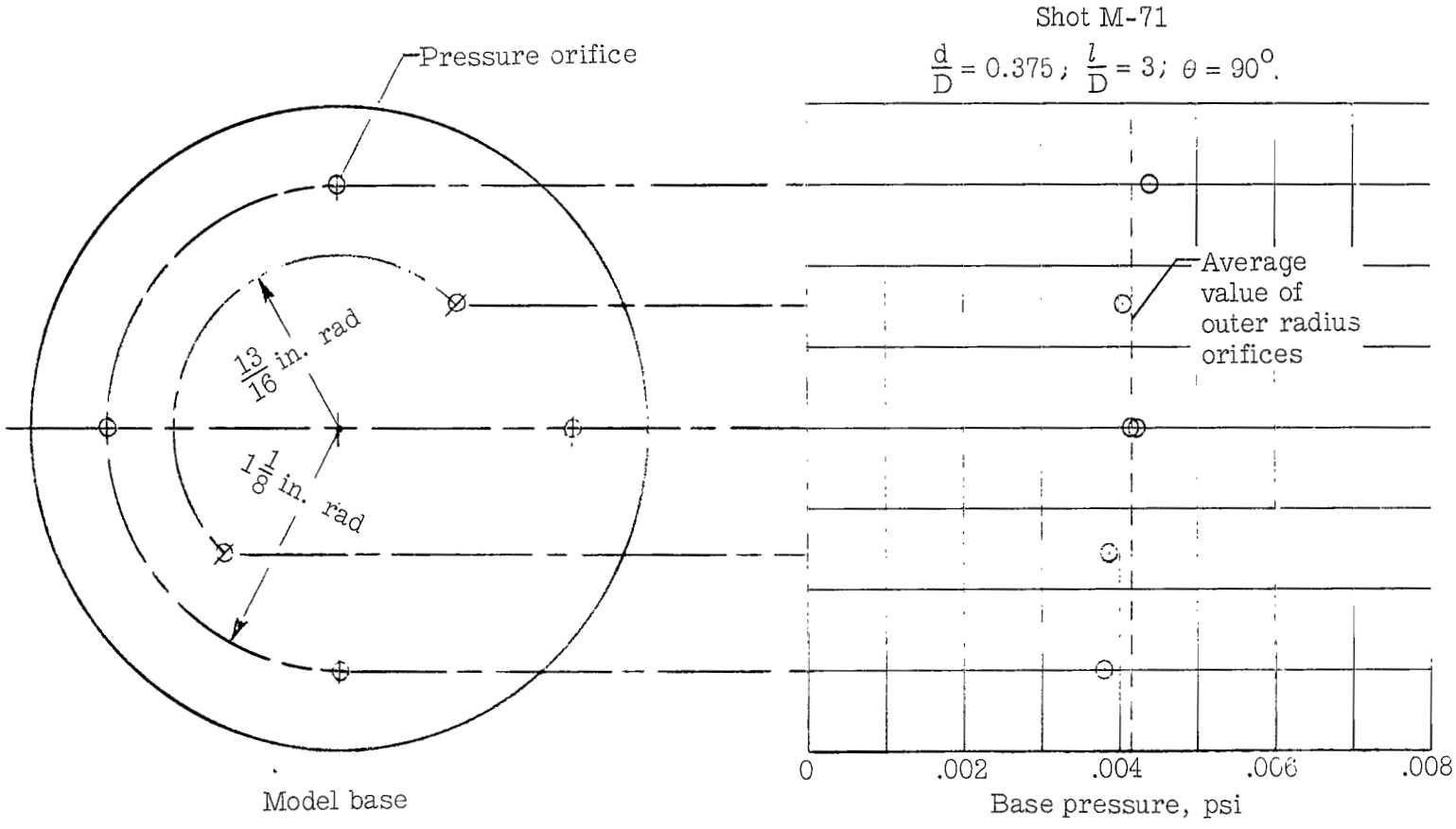

Figure 11.- Pressure distribution over model base.

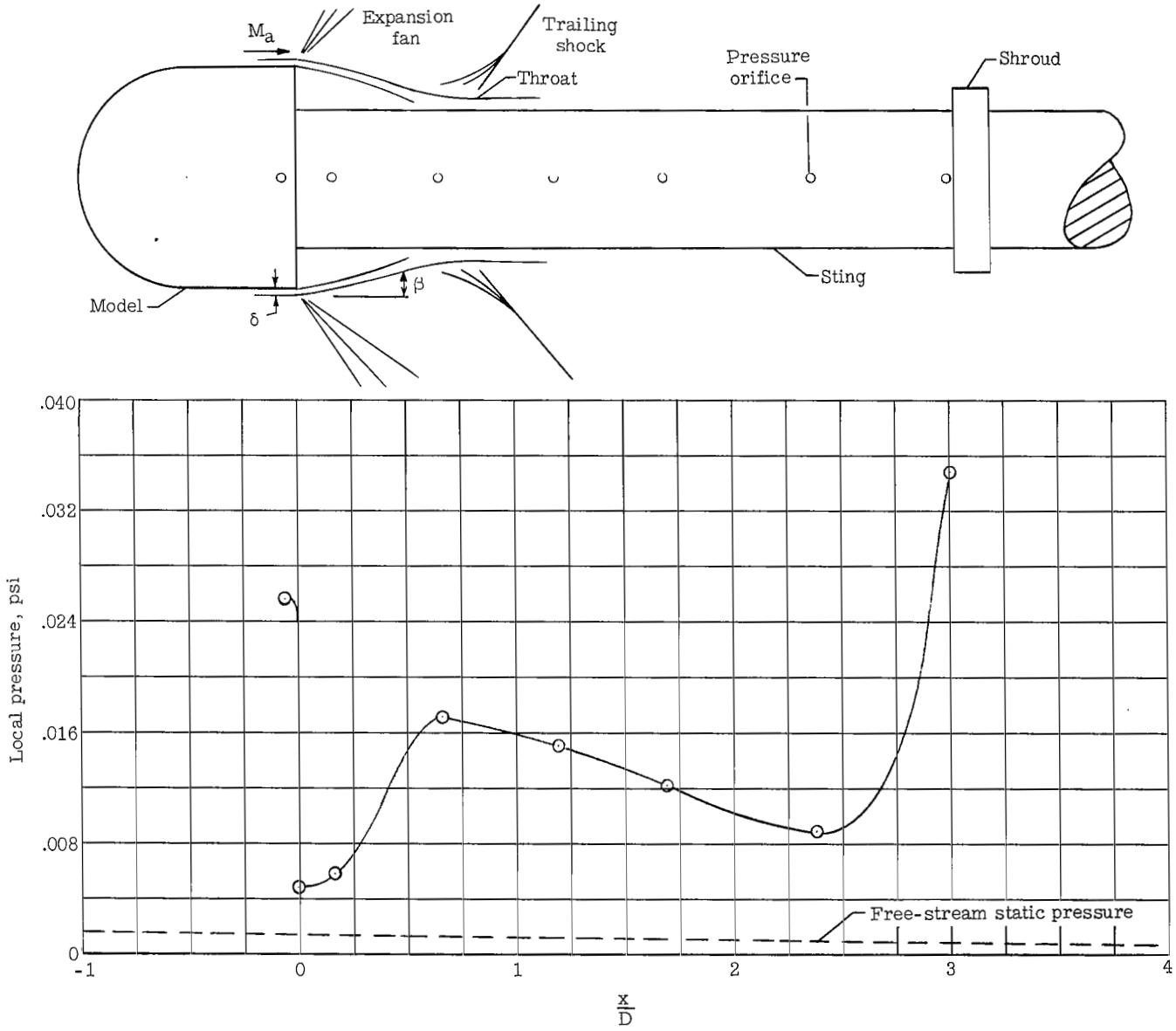

Figure 12.- Static pressure distribution ahead of base and along sting. $R_\infty = 4.65 \times 10^5$ per foot; $d/D = 0.625$; $l/D = 3$; $\theta = 90^\circ$.

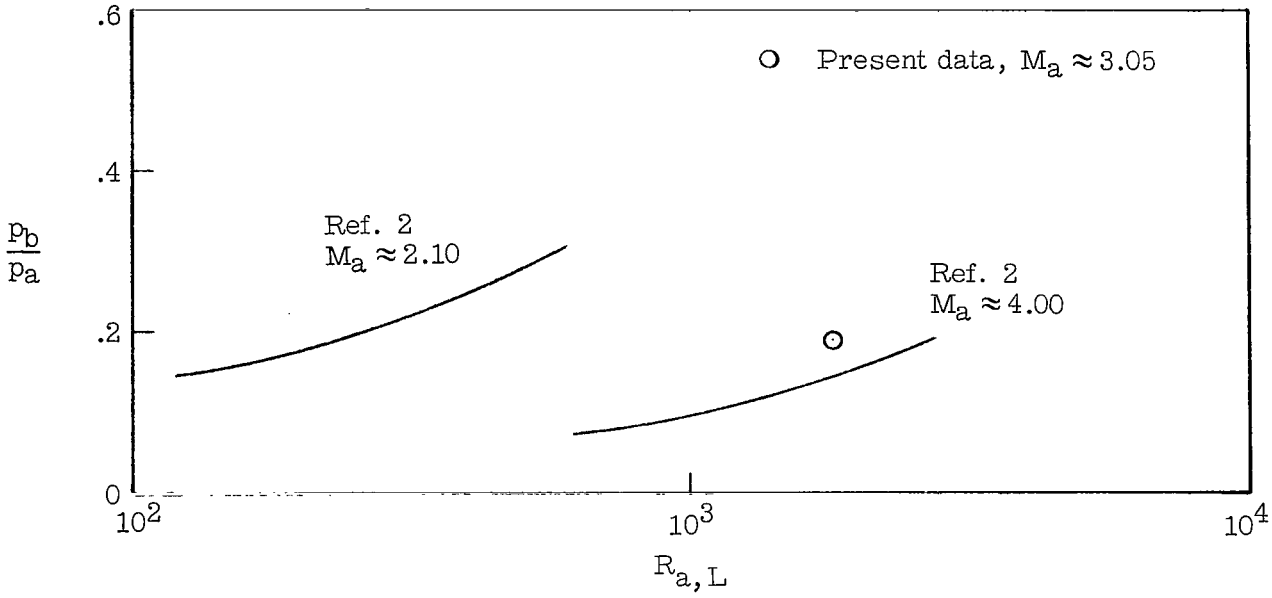

(a) Afterbody Reynolds number based on model length.

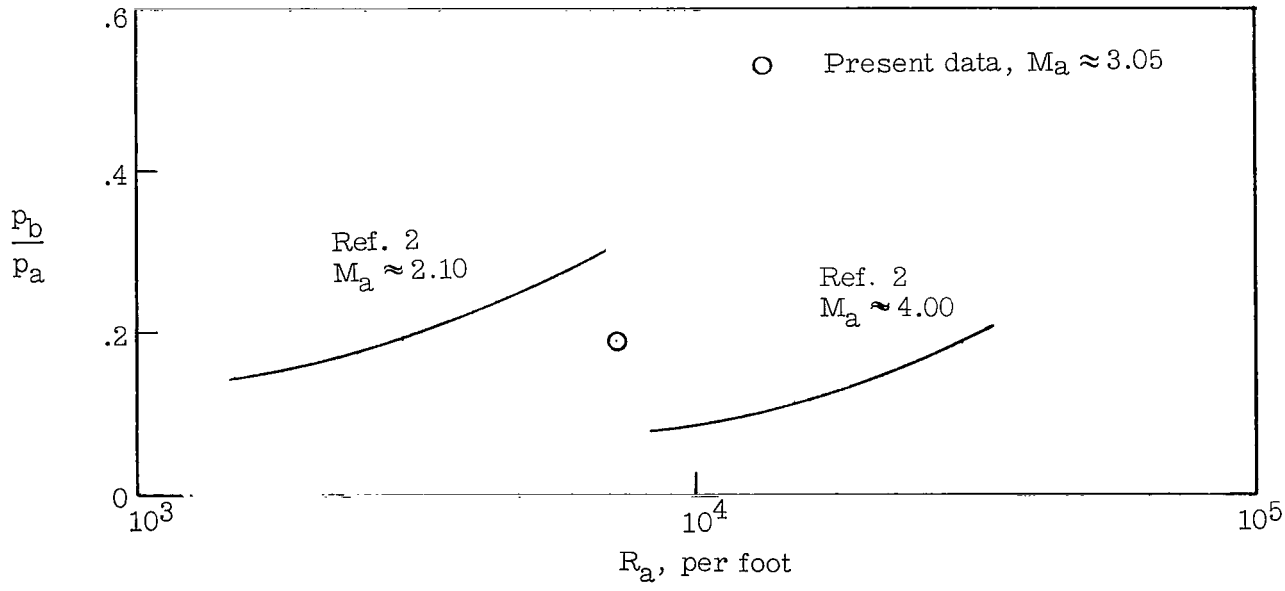

(b) Unit afterbody Reynolds number.

Figure 13.- Effect of Reynolds number on base pressure.

2/22/85
OR

"The aeronautical and space activities of the United States shall be conducted so as to contribute . . . to the expansion of human knowledge of phenomena in the atmosphere and space. The Administration shall provide for the widest practicable and appropriate dissemination of information concerning its activities and the results thereof."

—NATIONAL AERONAUTICS AND SPACE ACT OF 1958

NASA SCIENTIFIC AND TECHNICAL PUBLICATIONS

TECHNICAL REPORTS: Scientific and technical information considered important, complete, and a lasting contribution to existing knowledge.

TECHNICAL NOTES: Information less broad in scope but nevertheless of importance as a contribution to existing knowledge.

TECHNICAL MEMORANDUMS: Information receiving limited distribution because of preliminary data, security classification, or other reasons.

CONTRACTOR REPORTS: Technical information generated in connection with a NASA contract or grant and released under NASA auspices.

TECHNICAL TRANSLATIONS: Information published in a foreign language considered to merit NASA distribution in English.

TECHNICAL REPRINTS: Information derived from NASA activities and initially published in the form of journal articles.

SPECIAL PUBLICATIONS: Information derived from or of value to NASA activities but not necessarily reporting the results of individual NASA-programmed scientific efforts. Publications include conference proceedings, monographs, data compilations, handbooks, sourcebooks, and special bibliographies.

Details on the availability of these publications may be obtained from:

SCIENTIFIC AND TECHNICAL INFORMATION DIVISION

NATIONAL AERONAUTICS AND SPACE ADMINISTRATION

Washington, D.C. 20546